Journal of Power Sources, 5 (1980) 145 - 172

ELECTROCHEMISTRY, POWER SOURCES AND ENERGY SCIENCE*

ASHOK K. VIJH
Institut de recherche de l'Hydro-Québec, Varennes, Que. (Canada)
(Received October 25, 1979)

Summary

The scope of modern electrochemistry and its impact on energy science is outlined. Some of the important electrochemical interfaces encountered in energy device situations are described. Finally, a brief review of the current status of electrochemical power sources, *viz.*, fuel cells, batteries, and photoelectrochemical cells is presented.

1. Introduction

In the past couple of decades, electrochemistry has grown into a broad multidisciplinary science with many ramifications into problems bearing on energy research and development. Electrochemistry forms the basis of many power sources such as batteries and fuel cells. The scope of modern electrochemistry, however, encompasses several more areas of energy conversion, storage, and utilization technologies. The purpose of the present article is to focus on the structure of modern electrochemistry with a view of elucidating the manner in which electrochemical ideas and techniques are involved in the development of power sources and in the advancement of energy science.

2. The scope of modern electrochemistry

Modern electrochemistry comprises the study of ionic solutions and the science of the myriad phenomena occurring at the electrodes. The treatments of various problems in these two broad categories draw heavily upon (or interact strongly with) the following areas of scientific endeavour: chemical kinetics; theoretical electrostatics; solid state physics; heterogeneous catalysis; interfacial phenomena in charged interphases; metallurgy and materials

---

*Based on the 1979 Noranda Award Address of the Chemical Institute of Canada delivered by the author at the University of British Columbia on June 4, 1979 to the 62nd Canadian Chemical Conference.

An abstract version of this paper appeared in *Chemistry in Canada*, *32* (2) (1980) 28.

science; molecular biology and biomedical engineering; colloid and surface science; and, finally, instrumentation based on advanced electronics and optics. A convenient classification of the scope of modern electrochemistry is depicted in Table 1.

TABLE 1

Main areas of modern electrochemistry

(1) Ionic solutions and thermodynamics of electrolytes.
(2) Double layer and charged interfaces in general.
(3) Electrode kinetics and mechanisms of electrochemical reactions; theories of charge transfer.
(4) Electroanalytical chemistry.
(5) Applied electrochemistry: this will include research and development (at the laboratory level) in fields such as corrosion and protection of metals; electroplating, electrorefining and electrowinning of metals; batteries; fuel cells; electrolytic capacitors; electrochemical coulometers; electrochemical machining and electrosyntheses, etc.
(6) Electrochemical engineering: this constitutes the discussion of industrial processes or of pilot-plant projects in which principles of electrochemistry as well as engineering concepts are overlappingly involved.
(7) Interdisciplinary electrochemistry: for example in fields like colloids and surface chemistry, irreversible thermodynamics, bioelectrochemistry, biophysics, water pollution, ion exchange membranes and some aspects of solid state and materials science, knowledge of *both* electrochemistry and the other field is required for proper elucidation of the natural phenomena involved.

Although many of the above areas of electrochemistry contribute to the energy technologies in numerous ways, one of these areas stands out as the most prominent, namely, electrochemical physics: this is the advancing frontier where concepts of electrochemistry are combined with the notions of solid state science in order to develop better comprehension of problems associated with solid–electrolyte interfaces, solid electrolytes and derived applications [1]. The main fields of activity in electrochemical physics are listed in Table 2.

TABLE 2

General areas of electrochemical physics

Electrochemistry of semiconductors
Electrochemistry of insulators (*e.g.*, anthracene)
Anodic oxidation of metals
Reactions on demetallized surfaces
Electrocatalysis by metals
Role of crystal imperfections in metal deposition and dissolution reactions
Solid electrolytes: ice
Energy levels in solids and electrolytes
Electrobiophysics
Industrial implications

From the foregoing it is clear that modern electrochemistry requires an understanding of a variety of advancing areas of contemporary science and, reciprocally, enriches these areas by bringing to bear upon them the modes of thought and techniques of electrochemistry.

Although a scientific discipline can provide a rich and challenging area of curiosity-generated research, as indeed electrochemistry does, it acquires a deeper significance only if it provides a key to the solution of some vexing technological and social problems. Electrochemistry has had an important role to play in industrial processes since the time of Michael Faraday and appears to offer intoxicating possibilities for some problems of the future. In the present article, we touch upon the impact of electrochemistry in one applied area only, namely, the energy science.

3. Electrochemical excursions into energy science

Electrochemistry forms the basis of several areas of energy science and some of these areas are shown in Table 3. A synoptic commentary on these advancing frontiers of electrochemical energy science may be made here, although a detailed discussion of some selected themes (*e.g.*, power sources) will be presented in a subsequent Section.

Highly efficient electrochemical conversion of chemical fuels to electricity may be carried out through a type of continuous-feed primary batteries called fuel cells, as decribed previously [2]. These fuel cells, when combined with electrolyzers, provide a means of storing electricity, as discussed recently in a topical article [3]. This excellent paper also describes the possibilities of storing electricity in high energy-density batteries [3]. A field of intense current research interest is the area of photo-electrochemical conversion of solar energy to obtain either synthetic fuels or electricity [4].

TABLE 3

Electrochemistry and energy science

---

1. Energy devices
    - (i) Electrolysers (storage)
    - (ii) Fuel cells
    - (iii) High energy density batteries (storage)
    - (iv) Photo-electrochemical cells
2. Conservation of energy
    - (i) Corrosion and corrosion inhibition
    - (ii) More efficient industrial electrolytic processes
    - (iii) Recycling of metals
3. Nuclear energy and power engineering
    - (i) Corrosion prevention and decontamination in nuclear reactors
    - (ii) Final concentration of D_2O
    - (iii) Metal/plasma interfaces (nuclear fusion, electric arcs, circuit breakers, etc...)
    - (iv) Wetting of surfaces under high electric fields
4. Electrochemical energy conversion in human beings

The production of metals used in consumer goods involves an immense expenditure of energy. The loss of these metals by corrosion of, *e.g.*, cars, bridges, containers, and industrial equipment, etc., presents an energy waste that can be considerably diminished by a more wide-spread application of the electrochemical knowledge on corrosion and its inhibition.

Electrolytic processes are employed not only in the extraction of some metals from their ores, but also for the production of many industrial chemicals such as fluorine, chlorine, hydrogen, oxygen and sodium hydroxide. A better comprehension of the mechanisms of electrode reactions, and thus the development of more catalytic and stable electrodes, provides an avenue for the conservation of electrical energy used in these industrial processes.

Electrochemistry also forms the basis of some processes for the recycling of metals thrown away as "scrap", thus leading to some further energy conservation.

In the operation and routine maintenance of a nuclear reactor, one must deal with the problems of corrosion prevention and surface cleaning (decontamination) of the fluid circulation "loops", and electrochemistry is at the heart of such know-how. The final concentration of D_2O in 95% heavy water can be conveniently carried out by means of electrolysis. The metal/plasma interfaces encountered in electric arcs, circuit breakers and the laboratory work related to nuclear fusion can be treated quantitatively in terms of an electrochemical model [5]. The wetting of surfaces under high electric fields, as encountered in power engineering, is best examined in terms of electrochemical interfacial phenomena [6].

It has been suggested that the biochemical energy conversion in animals, including human beings, is electrochemical in nature [7]. Some pertinent facts indicating the validity of this position are summarized in Table 4.

TABLE 4

Biochemical energy conversion

Power equivalent of daily food consumption by a human being, assuming 100% efficiency of heat to mechanical energy	140 Watts
Carnot efficiency (with 10 K temp. difference inside the body) is 3%; power equivalent is →	5 Watts
Constant power needed to operate human circulatory system is estimated to be	10 Watts
High efficiency of energy conversion in humans implies an electrochemical mechanism, as also suggested by some mechanistic studies.	

4. Electrochemical interfaces in some energy device situations

The interfaces relevant to electrochemical energy science are those formed at the boundary of a typical electrode and an electrolyte (Table 5). The features of some of the more important interfaces are as follows:

TABLE 5

Electrochemical interfaces in some energy devices

Electrodes	Electrolyte (or "equivalent")
Metal	- Aqueous electrolyte
	- Non-aqueous electrolyte
Semiconductor	- Molten salt
	- Solid electrolyte
Demetallized surface	- Insulating liquid
	- Plasmas
	- "Vacuum"

NOTES:

(1) Plasmas are charged species in the gas phase and may best be treated as gaseous electrolytes [5].

(2) The word "equivalent" under the column on electrolytes refers to vacuum which in practice is a low-pressure plasma, *i.e.*, vacuum contaminated by charged micro-particles and ionic species released into the vacuum gap by the electrodes sustaining the vacuum under conditions typical of power engineering applications, *e.g.*, vacuum arcs, switches and circuit-breakers, etc.

(3) An electrode is essentially an electronic conductor whereas an electrolyte is an ionic conductor. Thus an insulating liquid is an electrolyte by virtue of ever-present impurity ions; similarly a vacuum is an electrolyte (gas phase) since it behaves as a low pressure plasma.

Metal–electrolyte interface

The most important aspect of the metal–electrolyte interface (Fig. 1) in the present context is the catalysis at electrodes of typical bonding reactions that may be involved, *e.g.*, in a fuel cell (see below) or an electrolyzer, *i.e.*, the subject of *electrocatalysis*: it attempts to explore the relationship between the properties of an electrode and the magnitude of its activity towards a given electrode reaction [1, 8 - 13]. In this sense, it is very similar to the field of gas-phase heterogeneous catalysis except for the presence of the following two additional parameters:

(i) The presence of a potential drop at the metal–solution interface can alter the energy of activation for the catalytic reaction in a given direction, depending on the sign and magnitude of the applied electrode potential.

(ii) The presence of a potential drop (and, hence, field) in the interphasic region between the electrode and the electrolyte creates a situation which tends to encourage, under some experimental conditions, the corrosion and dissolution of the electrode.

If one takes into account these additional factors of the potential drop and the electrochemical stability at the electrode–electrolyte interface, one realizes that many of the other factors involved in electrocatalysis are similar to those found in the theory of heterogeneous catalysis at metals. The purpose of this Section is to describe the elements of electrocatalysis.

Although there is a wide variety of electrode reactions that display a spectrum of interesting characteristics, it is sufficient to choose a simple

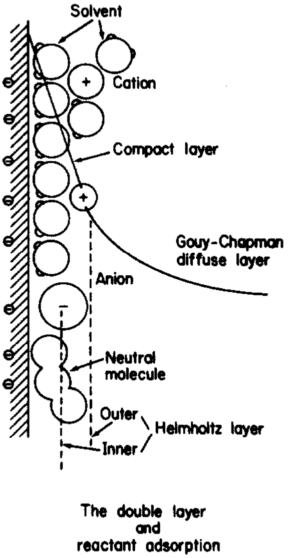

Fig. 1. A general representation of the double layer at a metal–electrolyte interface, with reactant (neutral molecule) adsorption; taken from Conway [12].

example to illustrate the essential principles involved, namely, the electrolytic (cathodic) evolution of hydrogen. It is generally called the hydrogen evolution reaction and denoted by HER. The HER is a model reaction for considering electrocatalysis since it is an example of a bonding reaction, *i.e.*, a reaction in which the reaction intermediates are strongly chemisorbed on the electrode, thus enabling the latter to display its catalytic characteristics, the same as in gas phase heterogeneous reactions. In acidic solutions, the overall HER, on a catalytic electrode such as Pt, may be represented as:

$$2H_3O^+ + Pt + 2e \rightarrow H_2 + 2H_2O \tag{1}$$

The various elementary steps generally believed to be involved in the overall reaction (1) are

$$H_3O^+ + Pt + e \rightarrow Pt\text{–}H + H_2O \tag{2}$$

followed by

$$Pt\text{–}H + H_3O^+ + e \rightarrow H_2 + Pt + H_2O \tag{3}$$

or

$$Pt\text{–}H + Pt\text{–}H \rightarrow H_2 + 2Pt \tag{4}$$

where e is the electron donated by the platinum cathode, H_3O^+ is the hydrated proton in the acidic aqueous solutions, and Pt–H represents a chemisorbed hydrogen atom on a site on the Pt electrode.

In an electrolysis experiment in which the hydrogen is being evolved at the cathode, the electrolysis current density, i (in A cm^{-2}), is the measure of the rate of hydrogen evolution because

$$i = ZFv \tag{5}$$

where v is the "chemical" measure of the rate of reaction (1), *i.e.*, moles of H_2 formed per cm^2 of the electrode surface; Z is the valence (*i.e.*, charge) of the species discharging on the electrode which, in the example of H_3O^+ chosen here, has a value of 1; F denotes the faraday, *i.e.*, 96 500 coulombs approximately (Note: 1 coulomb is equal to 1 ampere passed for one second). To get a net rate of reaction in an electrolysis experiment one forces a current, i (in a constant-current electrolysis arrangement), through the circuit which results in the evolution of hydrogen at the cathode and oxygen at the anode according to Faraday's laws of electrolysis, assuming that one is working with a typical set-up, *e.g.*, an aqueous sulphuric acid solution containing a platinum cathode and a platinum anode. The passage of current, i, displaces the potential of the electrode, cathode in our example, from its reversible value V_{rev} (for the reaction $H_3O^+ + e \rightleftharpoons \frac{1}{2}H_2 + H_2O$), to another value, V. The difference ($V - V_{rev}$) is the measure of irreversibility forced on the cathode by the passage of current density, i, and is called overpotential, η. If one conducts the experiment under conditions of controlled electrode potential (*i.e.*, potentiostatic electrolysis configuration) one has to apply the overpotential, η, to force the current, i, through the electrolysis circuit. The overpotential, η, is thus the driving force externally applied to the working electrode and is needed to sustain the electrode reaction at a given rate. The higher the value of this driving force for obtaining a given rate of hydrogen evolution, the worse is the catalytic property of the electrode for the HER. For a good electrocatalyst such as Pt, negligibly low values of η are needed to effect rather high rates of HER. The η and i are related by the Tafel equation:

$$\eta = a - b \log i \tag{6}$$

where a and b are constants characteristic of the electrode material. When the value of the overpotential is zero, it means that the driving force for the reaction is zero and that one is operating at the reversible potential. Under these conditions, the rate i assumes its lowest possible value, *i.e.*, its value at the reversible potential; this value of i is called the exchange current density, i_o, and is a measure of the rate of dynamic equilibrium at the reversible potential. Since at the reversible potential the driving force, η, is zero, one cannot have a net electrode reaction, thereby creating a situation in which a dynamic equilibrium is sustained at the reversible potential. Thus,

$$i_o = \overrightarrow{i} = \overleftarrow{i}. \tag{7}$$

In other words, the forward rate $\overrightarrow{i}$ equals the backward rate $\overleftarrow{i}$ (of, *e.g.*, reaction (1)) and each of these rates is equal to the exchange current density, i_o. This i_o is usually taken as the measure of the intrinsic electrocatalytic activity of a given metal in an electrode reaction. It is observed that the values of i_o for the HER on various metals show a very large variation; *e.g.*, on Hg, in highly acidic concentrated solutions, the i_o for the HER is around 10^{-13} A cm^{-2} whereas for smooth platinum, it lies in the neighbourhood of 10^{-3} A cm^{-2}. The subject of electrocatalysis is then reduced to the essential question: What properties of metals and other factors are responsible for different i_o values for the HER (or for any other chosen reaction) on different metals ?

In electrode reactions such as hydrogen evolution, the presence of adsorbed reaction intermediates is indicated, at least for the more catalytic metals. The evidence for the presence of adsorbed intermediates during the electrode reaction is principally deduced from electrochemical transient studies, *e.g.*, open circuit decay of electrode potential, potentiodynamic (*i.e.*, cyclic voltammetric) profiles, charging curves (*i.e.*, chronopotentiograms), and by a combination of a variety of potentiostatic and galvanostatic pulse techniques. Recently-developed optical techniques also provide useful information on the coverage of the electrode by adsorbed species during the electrode reaction. In any case, these gas evolution and dissolution reactions are influenced profoundly by a number of solid state properties of metallic electrodes, *e.g.*, work functions, heats of sublimation and the metal–metal (M–M) bond energies derived therefrom, electronegativities, electronic structure of metals (especially in relation to unfilled d-bands in transition metals), lattice parameters, and a variety of other quantities such as atomic number, compressibility, density, ionization potential, melting point, boiling point, hardness, volume and linear expansion, ionic radius, electrical resistance, etc.

An examination of the influence of these properties on the electrocatalysis of a typical electrode reaction, *e.g.*, hydrogen evolution reaction (HER), by metals would show that all these properties determine the electrocatalytic tendencies of metals by virtue of their effect on the strength of the M–H binding of an adsorbed hydrogen atom, H, on a metal site, M. Theoretical treatments of the role of M–H interaction energy in the electrocatalysis of the HER by metals involve the following essential rate equations:

The forward rate equations for the steps in eqns. (2) and (3) are, respectively:

$$i_2 = \frac{kT}{h} \mathrm{F}(1-\theta)C_{\mathrm{H_3O^+}} \exp\left\{-\frac{\Delta g_o}{RT} - \frac{\beta \Delta G_{\mathrm{H}}}{RT} - \frac{\beta \mathrm{F} E}{RT}\right\} \tag{8}$$

and

$$i_3 = \frac{kT}{h} \mathrm{F}\theta C_{\mathrm{H_3O^+}} \exp\left\{-\frac{\Delta g'_o}{RT} + \frac{\beta \Delta G_{\mathrm{H}}}{RT} - \frac{\beta \mathrm{F} E}{RT}\right\}. \tag{9}$$

Here, Δg_ρ and $\Delta g'_o$ are the adsorption-independent (*i.e.*, metal-independent) free energies of the activated complex at $E = 0$, where E is the electrode potential measured against an arbitrary reference electrode; ΔG_{H} is the free energy of adsorption of atomic hydrogen, H; i_2 and i_3 are the current densities; k, T and h are Boltzmann constant, absolute temperature and Planck's constant, respectively; θ is the fraction of the electrode surface covered by adsorbed H; $C_{H_3O^+}$ is the bulk concentration of the H_3O^+ ions and, for simplicity of discussion, may be taken as the surface concentration by assuming concentrated solutions; R is the gas constant; F is the Faraday; and β is the charge transfer symmetry factor with the usual value equal to 0.5.

It should be emphasized here that the electrocatalytic activity of an electrode in the above rate equations is governed by the magnitude of ΔG_H, which, in turn, is determined by the physical and electronic properties of the metals, as mentioned above.

(B) Semiconductor–electrolyte interface

The central difference between electrode reactions on metals and on semiconductors is that in the latter, the kinetics of the reaction may depend on processes that occur within the solid electrode [1, 14 - 18]. The rate of the reaction may depend, for example, upon the rate of supply of minority carriers to the semiconductor surface, assuming that they are consumed in the reaction. The rate of generation of these carriers, of course, depends on the bending of the bands near the surface, *viz.*, on the potential drop across the space charge region (Fig. 2).

In order to investigate the characteristic effects of the semiconductor electrode on the kinetics of charge transfers across semiconductor–solution interfaces, it is best to work in concentrated electrolyte solutions so that the potential drop across the diffuse double layer on the solution side is negligible. With this restriction and for the case of a semiconductor–electrolyte interface, almost all the applied electrode potential operates across the space charge region within the semiconductor and there is hardly any change in the potential drop across the Helmholtz double layer with the changes in the total applied electrode potential. In order to derive the typical kinetic equations for such a case, one may consider a reaction of the type

$$A + e \rightarrow A^- \tag{10}$$

where the rate is first order with respect to electron concentration on the surface, *i.e.*, in the reaction zone.

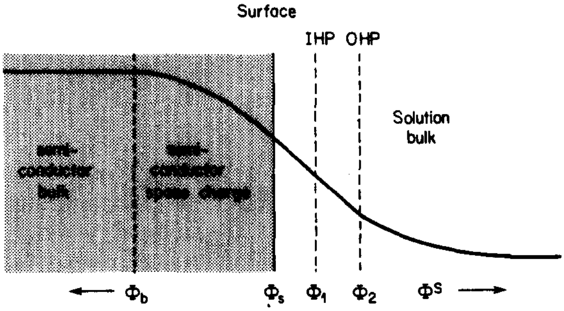

Fig. 2. Model of the semiconductor–electrolyte interface, after Boddy [17].

The surface concentration of the electrons, n_s, in a semiconductor is related to their bulk concentration, n_o, by the equation:

$$n_s = n_o \exp(-e(\phi_b - \phi_s)/kT) \tag{11}$$

where $\phi_b - \phi_s$ (Fig. 2) is the magnitude of the potential drop across the space charge region within the semiconductor. For the simple case assumed here, then, the rate of reaction or the current density, i, is given by

$$i = [A] n_o \exp(-e(\phi_b - \phi_s)/kT). \tag{12}$$

On taking logarithms and differentiating, assuming $[A]$ and n_o as constants, we obtain,

$$\frac{\partial(\phi_b - \phi_s)}{\partial \log i} = -2.3 \frac{kT}{e} \approx \text{pseudo-Tafel slope.}$$

Similarly, if the reaction rate is of the first order in hole concentration, one would analogously obtain the rate equation

$$i \propto p_o \exp(e(\phi_b - \phi_s)/kT) \tag{13}$$

and the corresponding pseudo-Tafel slope will be again,

$$\frac{\partial(\phi_b - \phi_s)}{\partial \log i} = 2.3 \frac{kT}{e}.$$

Whenever saturation currents limit the speed of the electrode reaction on a semiconductor, illumination of the electrode surface with light of energy higher than the band gap value increases the rate of the electrode reaction. Such an increase of the reaction rate occurs because illumination decreases the $(\phi_b - \phi_s)$ potential drop by exciting electrons from valence to conduction band at the surface.

The photo-electrochemical cells utilizing semiconducting electrode materials and aimed at converting solar energy either to electrical energy or to chemical fuels (*e.g.*, H_2, CH_3OH) are an area of intense current research work [4].

It should be emphasized here that in addition to the simple case of an electrode reaction on an "idealized" semiconductor electrode, several other complex cases can arise that require more elaborate kinetic treatments. These cases have been developed previously both in the absence and presence of photo-effects [14 - 19].

(C) Demetallized surface–electrolyte interface

A vast number of electrode reactions, proceeding nominally on a metallic electrode, occur, in fact, on an electrode surface which is covered by a semiconducting solid electrodic layer, *viz.*, a demetallized surface (Fig. 3). This is particularly true of all reactions (including cathodic ones, *e.g.*, reduction of oxygen) that take place at potentials anodic to that of the hydrogen electrode. In such cases, the electrode surface sustaining the electrode reaction is a semiconducting layer attached to the substrate metal. The electrode

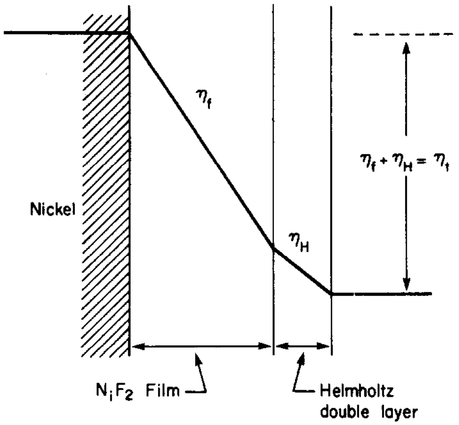

Fig. 3. A schematic representation of the potential drops across demetallized surface–electrolyte interface comprising a NiF_2 - covered Ni electrode being anodized in AHF [22].

kinetic behavior of such electrodes is dictated by the solid state properties, especially the semiconductivity, of the solid layer rather than by the properties of the underlying metal [1, 14, 20 - 22]. The thickness of such films can range from about 10 Å (as, *e.g.*, on Pt under *ordinary* conditions of anodic polarization) to about several thousand angstroms, the latter being the case for the so-called valve metals, *viz.*, Al, Ta, Nb, Ti, Hf, Zr, etc. It is clear, therefore, that oxide films of several atomic layer thickness can be formed on all metals under suitable conditions.

In the case of a semiconducting film on a metal, one may approximate the film to a bulk semiconductor and thus proceed to apply the kinetic analysis appropriate for semiconductor electrodes. However, when one equates the behavior of a film-covered metal with that of a semiconductor, one needs to prove that the Debye length (*i.e.*, the effective thickness of the space charge region) of the surface film is less than the thickness of the film itself. The Debye length is given by the formula:

$$L_D = \left(\frac{\epsilon kT}{4\pi ne^2} \right)^{1/2} \tag{14}$$

where L_D is the Debye length of the semiconducting film covering the metal; ϵ is the dielectric constant of the film, k is the Boltzmann constant; T is the absolute temperature, n is the density of electronic charge carriers and e is the electronic charge. For high densities (*ca.* 10^{19} - 10^{20} carriers cm^{-3}) of charge carriers (not unusual in the surface films of demetallized surfaces) and a reasonable value of dielectric constant (*ca.* 50), one can, in fact, deduce L_D values close to 10 Å, although it is somewhat debatable that the semiconductor space charge theory can be strictly applied to these cases.

It should also be noted that many of the electrodic films are amorphous in character so that they essentially behave as intrinsic semiconductors even when containing impurities, which, in the case of *crystals* of the same composition, act as donors or acceptors. It is not necessary, therefore, to take into account the role of surface states in dealing with reactions on film-covered electrodes.

The demetallized electrodes can be involved in many electrochemical situations pertinent to energy science, *e.g.*, fuel cells, electrolyzers, corrosion and dissolution of metals etc.

(D) Metal/plasma interface

An important aspect of research and development in energy science is the area of transmission and distribution of electrical energy. Here, power engineers and scientists encounter several problems associated with electrical contacts, switches, circuit breakers, and electric arcs in which metal/plasma interfaces are involved. Also, the nature of metal/plasma interfaces is of central interest for the advancing body of knowledge needed to harness nuclear fusion — the ultimate, inexhaustible source of energy for the future. Electrochemical concepts provide a means to calculate some basic parameters at the metal/plasma interfaces and yield a framework for understanding some of the problems pertinent to such interfaces [5, 23]. An electrochemical approach to the magnitude of the so-called cathode fall at metal–plasma interface is as follows (Fig. 4).

In an arc the metal erodes from the cathode giving cations, M^+, and electrons, *e*. The univalent cation M^+ may subsequently, in the plasma medium, undergo further successive ionizations to give M^{2+}, M^{3+}, M^{4+} ... M^{z+} depending on the nature of M^+, its chemical identity, and the conditions prevailing in the plasma. The potential drop developed at the M/M^+ interface is called the cathode fall and operates over a distance of a few thousand angstroms. This erosion process may be treated as the electrochemical dissolution to yield M^+ from the metal surface. In the electrochemical dissolution of a

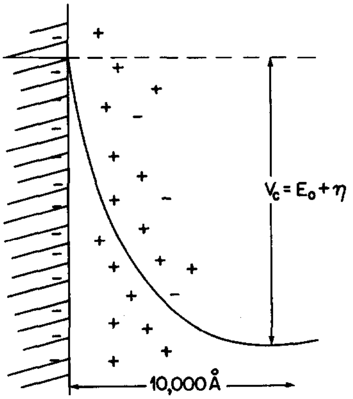

Fig. 4. A schematic diagram of the potential profile across a typical metal/plasma interface as may be encountered, *e.g.*, in an electric arc [5]. Here, V_c is the so-called cathode fall (see the text), η is the overpotential and E_0 is the reversible potential for the electrochemical equilibrium pertaining to this situation.

metal in an electrolyte solution, the process involved is also (assuming a univalent cation, for simplicity of arguments) the same as in the arc, *i.e.*,

$$M \rightarrow M^+ + e. \tag{15}$$

However, in the electrolyte solution, the M^+ undergoes hydration (in the aqueous electrolyte) or appropriate solvation (in a non-aqueous electrolyte) and the electrode potential is given (on the hydrogen electrode scale arbitrarily chosen by electrochemists) by:

$$eE^o = \Delta G_A + \Delta G_I + \Delta H_h \tag{16}$$

where ΔG_A is the free energy of atomisation of the metal, ΔG_I is the free energy of ionization (*i.e.*, the ionization potential) of the gaseous metal atom to give the metal ion, and ΔH_h is the heat of hydration of the ion (assuming we are working in an aqueous electrolyte); e is the electronic charge. E^o is in units of volts whereas ΔG_A, ΔG_I and ΔH_h are in electron-volts.

For the reaction at the metal/plasma interface, the cation formed in eqn. (15) does not undergo hydration but stays as a cation. Hence, for this case, eqn. (16) becomes:

$$eE^o = \Delta G_A + \Delta G_I. \tag{17}$$

Here E^o is the reversible thermodynamic potential for the reaction in eqn. (15). According to the theory of electrode reactions, at the reversible potential, E^o, no net reaction can take place and reaction (15) is in equilibrium as:

$$M \rightleftarrows M^+ + e.$$

In order to effect the net rate of reaction in eqn. (15), it is necessary to exceed E^o and develop some overpotential, η, which drives the equilibrium reaction in the forward direction, *i.e.*, conversion of M to ($M^+ + e$). Since V_c refers to the cathode fall (expressed in units of eV) when net reaction (15) proceeds at detectable rates, then it follows that

$$V_c = e(E^o + \eta). \tag{16}$$

In order to develop the above argument further, it is necessary to consider two additional points:

(i) Based on the work of Grakov, it now appears that the magnitude of the cathode fall increases negligibly with even substantial increase in the arc current values. In other words the overvoltage, η, values have small magnitudes for arc electrode reactions and are negligible as compared to the E^o values. One may, therefore, write eqn. (16) as

$$V_c \approx eE^o. \tag{17}$$

It should be pointed out that in view of the analogous cases of metal deposition–dissolution reactions which are very fast (and, hence, negligible η) for several metals in suitable electrolyte solutions, it is not entirely surprising that the η values for the gas-phase "metal dissolution" as from the cathode of an arc, are of almost vanishing magnitude.

(ii) Since the difference in the Fermi energy of the electron in metal and in vacuum (*i.e.*, the work function, ϕ) for every metal has different values, it now appears that the E°_{rev} for the metal–vacuum interface for every metal should not be taken as zero but will be equal in magnitude to the work function, ϕ, for every metal.

One will thus have

$$V_c \approx eE^{\circ} + eE^{\circ}_{\mathrm{rev}} \approx eE^{\circ} + \phi . \tag{18}$$

The cathode fall, V_c values, thus calculated by eqns. (17) and (18) are given by

$$V_c \approx \Delta G_A + \Delta G_I + \phi . \tag{19}$$

Very good agreement between the theoretical values of V_c, as given by eqn. (19), and the experimental values has, indeed, been observed [23].

5. Some electrochemical power sources

Electrode reactions form the basis of both the electrochemical power producers (*e.g.*, fuel cells and batteries) and the electrochemical power consumers, *i.e.*, electrolyzers; in photo-electrolysis, the two functions can, however, be combined in some appropriate situations. Electrolyzers as such will not be discussed here since the focus is on the power sources only.

(A) Fuel cells

Fuel cells are continuously -fed primary batteries in which the appropriate chemical substances are "consumed" at electrodes to produce electricity. The direct conversion of chemical energy to electrical energy will continue to proceed in a fuel cell as long as the reactants ("fuels") are being fed into it and the products of the electrode reactions are being eliminated from the device.

To illustrate the principles involved in a typical fuel cell, consider a hydrogen–oxygen fuel cell. In its barest essentials, it involves an anode and a cathode immersed in an electrolyte. Gaseous hydrogen is fed at the anode and gaseous oxygen (or air) is led onto the cathode. The anodic and cathodic reactions involved in an acidic electrolyte are

$$\text{anode} + H_2 \rightarrow \text{anode} + 2H^+ + 2e^- \tag{20}$$

$$\underline{\text{cathode} + 1/2\, O_2 + H_2O + 2e^- \rightarrow \text{cathode} + 2OH^-} \tag{21}$$

$$H_2 + 1/2\, O_2 \rightarrow H_2O \tag{22}$$

The overall reaction in the fuel cell is given by combination of the anodic reaction and the cathodic reaction and is the electrochemical "combustion" of H_2 and O_2 to form H_2O. The waste product in this particular example of the fuel cell is the H_2O which must be continuously removed. As a result of the reactions in eqns. (20) and (21), the anode and cathode will acquire a difference of potential derived from the free energy change in the overall reaction in eqn. (22).

The intensity (the difference of the reversible potentials of the anodic and the cathodic reactions, denoted by E, in volts, V) and the quantity (in faradays, F, or coulombs, C) of the total fuel cell output are contained in the molar free energy change, ΔG, of the overall reaction eqn. (22). The relationships between these diverse quantities are given by

$$\Delta G = -n\mathrm{F}E = -E\int I dt = \mathrm{VC} \tag{23}$$

where n is the number of electrons per molecule of the anodic fuel (for hydrogen in the present example, n is, of course 2), I is the average current in amperes derived for t seconds. In addition to a large variety of highly sophisticated engineering problems associated with the fabrication of a practical fuel cell, the major fundamental problem is the rather slow rates of reactions such as in eqns. (20) and (21) under conditions of load, especially when economically-preferable fuels are used instead of hydrogen. The ideal solution would appear to be the discovery of stable, inexpensive, and abundant electrocatalysts which can catalyze these reactions to high rates.

For the cathodic reaction, oxygen in air is obviously a readily available inexpensive fuel provided that a suitable electrocatalyst for its reduction at high rates can be found. If the anode and the cathode in the fuel cell are not good electrocatalysts, electricity-producing reactions proceed at significant rates only if large fields develop across the electrode–electrolyte interfaces to force these activation-controlled reactions; this situation is unacceptable in a practical fuel cell since activation polarization across the anode and the cathode leads to high power losses. Poor electrocatalysts thus give rise to a power loss because a significant fraction of the potentially available output voltage of the fuel cell battery is wasted in driving the battery reactions instead of the external load. The search for inexpensive cathodic electrocatalysts has been directed to bronzes, phthalocyanines, and other organic semiconductors, and a variety of semiconducting oxides [1].

The hydrogen fed into a hydrogen–oxygen fuel cell is usually provided by the catalytic decomposition of a common fuel such as methane or propane in a reformer. The most familiar type of such a fuel cell uses phosphoric acid as the electrolyte and operates around 200 °C. The electrocatalyst is highly-dispersed platinum carried on a porous graphite substrate. There are several other types of fuel cells that employ other electrodes or electrolytes and/or operate at higher temperatures [11, 13]. The technological effort aimed at producing commercial fuel cells is mainly being directed at two types, namely, the phosphoric acid and the molten carbonate, although some other types of fuel cells are also claimed to offer great promise by their respective proponents.

In order to obtain some idea of the current status of technology in this field, we draw upon the excellent recent evaluations of Fickett and coworkers [24 - 26]. Based on the most recent report by Fickett [26], the current technological targets for these devices are as in Table 6; the present

TABLE 6

Fuel cell program targets [26]

	First generation	Advanced technology	
Installed cost (1978 $/kW)	300 - 400	300 - 400	800 - 900
Efficiency	37%	45%	45%
Endurance (h)	40 000	40 000	40 000
Fuel capability	Lt. distillate Methanol Syn. gas Natural gas SNG	Distillate Methanol Syn. gas Natural gas SNG	Coal (integrated with a gasifier)
Technology	Phosphoric acid	Advanced phosphoric acid or molten carbonate	
Commercial availability	1985	1990	1995

status of the phosphoric acid and the molten carbonate technologies is presented, respectively in Tables 7 and 8. The cell voltage–current density characteristics of these two types of fuel cells are shown in Fig. 5 [26].

It is also interesting to summarize, after Fickett [25], the major fuel cell projects, as in Table 9. In this table, TARGET stands for Team to Advance Research for Gas Energy Transformation and this program was supported by the gas-utility industry; the FCG (for fuel cell generator) program was originated by the electric-utility industry. Both these programs were carried

TABLE 7

Phosphoric acid technology status [26]

First generation requirements
- 37% efficiency is readily achieved
- Efforts required to achieve 40 000 hours of electrolyte inventory
- 1 MW pilot plant operated for 1 000 hours
- 4.5 MW demonstrator will be tested in 1980

Advanced technology requirements
- 45% efficiency is difficult
- Will require significant improvements to O_2 electrode

TABLE 8

Molten carbonate technology status [26]

Advanced technology requirements
- 45% efficiency achievable in small cells
- Largest unit operated to date is 1 kW stack
- Efforts required to achieve 40 000 hours
- Electrolyte integrity and inventory
- Electrode stability
- With low cost materials and processes

TABLE 9

Major fuel-cell projects [25]

Project	Function	Duty	Size	Fuel	Cost 1980 US	Efficiency	Available	Electrolyte
TARGET	On-site power-plants	Load following (continuous)	25 - 200 kW	Natural gas	$ 500	35 - 40 (100)	Early 1980's	Phosphoric acid
FCG-1	Dispersed power-plants	Load following (intermediate)	10 - 25 MW	Naphtha	$ 350	37 - 39 (75 - 80)	Early 1980's	Phosphoric acid
UTILITY	Dispersed power-plants	Load following (intermediate)	10 - 25 MW	Petroleum or coal derived liquids	$ 350	45 - 47 (75 - 80)	Late 1980's	Molten carbonate or phosphoric acid
UTILITY	Central power-plants	Base load	150 - 600 MW	Coal	$ 800	45 - 47	1990's	Molten carbonate or phosphoric acid

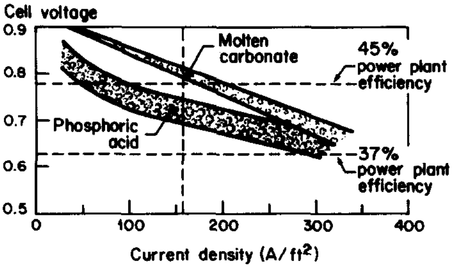

Fig. 5. The cell voltage–current density characteristics of the phosphoric acid and molten carbonate fuel cells at the level of their technology in early 1979, after Fickett [26]. (Ordinate × 10 (approx.) to give A/m^2.)

out by the United Technologies Corporation of U.S.A. The programs in Table 9 labelled under utility signify long-range plans by the electric-utility industry. The cost refers to the 1980 U.S. dollar. The efficiency figures on the upper line represent plants without recovery of waste heat, whereas those on the lower line (in parentheses) pertain to plants which include equipment for recovering waste heat.

(B) Batteries

There are several classes of batteries although distinction between these various classes is not always rigid. In *primary* batteries, when the reactants (including one or both electrodes) initially put in them are consumed by the electricity-producing electrochemical reactions, the battery is discarded; *i.e.*, after the battery is discharged, the chemical products cannot be brought back to their initial (*i.e.*, before discharge) reactant form by charging. A familiar example of such batteries is the mercury cell. The *secondary* battery is one which can be charged and discharged several times. During discharge, the electricity-producing electrochemical reactions cause changes in the composition of the electrodes and the electrolyte; during charging, these changes can be reversed back to restore the original conditions. A familiar example of such batteries is the lead–acid battery. Whereas the primary batteries, strictly, must be regarded as the electrochemical energy conversion devices (like the fuel cells), the secondary batteries are true energy-storage units.

Advanced, high-energy secondary battery systems are being developed for electrical energy storage applications in electric automobiles and for utility peaking needs. Batteries for automobiles should possess high specific energy (kJ/kg) for maximum range, and high specific power (W/kg) for good acceleration; in addition, they must have long life-time and an acceptable initial cost. For the stationary energy storage required by electrical utilities, cost and life-time are more important, whereas high specific energy and specific power are less critical; however, these batteries must withstand cycling between fully-charged and fully-discharged states likely to occur in utility storage facilities.

For the load-levelling batteries, the required performance and cost goal is compared with these features available in current deep-cycling lead–acid batteries in Table 10, taken from an assessment of Birk, Klunder and Smith [27]. A similar comparison for the electric vehicle batteries is given in Table 11 [27]. A detailed comparative analysis of the features of the advanced high-energy batteries under intense current development is presented in Table 12 [27]. The major advanced battery programs in the U.S., together with the level of their funding, are listed in Table 13.

TABLE 10

A comparison of the performance and cost goals for the load-levelling batteries with those of deep-cycling industrial lead batteries [27]

Parameter	Goal	Lead–acid
Cost ($/kW h (1978 $))	40	80
Life (cycles)	>2 000	1 750
Life (years)	>10	8
Energy efficiency (ratio of ac discharge energy to charge energy) (%)	70	70
Footprint (6-m stacking) (kW h/m^2)	88	88
Charge time (h)	4 - 7	6 - 8
Discharge time (h)	3 - 10	5 - 10
Environmental impact	Nil	Nil

TABLE 11

A comparison of the performance and cost goals for electric vehicle batteries with those of existing lead–acid batteries used in golf carts [27]

	Goal	Lead–acid
Discharge time (h)	2 - 4	2 - 4
Charge time (h)	1 - 6	6 - 8
Energy density (W h/kg)	140	26
Power density-peak (15 s) (W/kg)	200	80
Power density-sustained (W/kg)	70	30
Volume energy density (W h/l)	200	50
Life (years)	10	5
Life (cycles)	800	300
Energy efficiency (ratio of discharge energy to charge energy) (%)	50	65
Typical size (kW h)	20 - 50	20 - 40
Cost ($/kW h)	40	45

Since there are many types of battery systems under investigation and all of them have advantages and drawbacks, it is extremely difficult to judge as to which system is the "battery of the future", either for electric vehicles

TABLE 12

The characteristics, projected cost, and test date estimates for the advanced batteries being considered as candidates for load-levelling application [27]

	Lead–acid (Pb/PbO_2)	Sodium–sulphur (Na/S)	Lithium–metal sulphide (Li/FeS_2)	Zinc–chlorine (Zn/Cl_2)
Operating temperature (°C)	20 - 30	300 - 350	400 - 500	25 - 50
Electrolyte	Sulphuric acid	Ceramic	Molten salt	Aqueous zinc chloride
Design modular energy density (W h/kg)	20	44	53	84
Design modular volumetric density (W h/cm^3)	0.046	0.06	0.049	0.06
Utilization of active material, during charge/discharge (%)	25	85	80	100
Current density (5 h discharge) (mA/cm^3)	10 - 15	100	30	40
Active materials cost ($/kW h)	8.5	0.49	4.27	0.74
Operating potential (V)	1.9	1.8	1.4	1.9
Battery size goal (kW h)	>20	10	40	50
Cell life goal (cycles)	>2 000	1 300 (30 W h)	1 000 (150 W h)	800 (1.7 kW h)
Costly or critical materials	Lead	None	Lithium	Graphite
Projected test date for 5-MW h system	–	1984	1985	1981

NOTE: The data on energy density and volumetric energy density represent different cooling arrangements for different batteries: water cooling for lead–acid; gas cooling for sodium–sulphur and lithium–metal sulphide; and a refrigeration system for zinc chloride. Liquid-cooled designs for sodium–sulphur enhance their energy density by about 40 - 50 (%).

TABLE 13

The major advanced battery programs in the U.S.A. [27]

System	Major developers	Estimated 1979 funding (10^6 $)	Major sponsor
Sodium–sulphur	Ford Motor Co., Newport Beach, Calif.;	4.8	DOE
	General Electric Co., Schenectady, N.Y.;	4.5	EPRI
	Dow Chemical Co., Walnut Creek, Calif.	2.0	DOE
Lithium–iron sulphide	Argonne National Lab., Argonne, Ill. (with subcontractors of Rockwell International, Canoga Park, Calif.; Gould Inc., Rolling Meadows, Ill, and Eagle Picher, Joplin, Mo.)	6.2	DOE
Zinc–chlorine	Energy Development Assc., Madison Heights, Mich. (a G&W company)	6.0	EPRI/DOE
Zinc–bromine	Gould Inc.	0.6	EPRI/DOE

NOTES: (1) EPRI denotes Electric Power Research Institute, U.S.A.: (2) The DOE is the Department of Energy, U.S.A.

or for load levelling. An attempt has been made recently to summarize the essential qualitative features of various contending battery systems currently being investigated in the U.S.A. [28] and this synoptic summary is given in Table 14.

Among the three high energy-density batteries in Table 12, Li–metal sulphide has the highest energy density but suffers from more severe problems of materials stability and corrosion owing to its quite high operating temperature; these problems, however, are not unmanageable. The sodium–sulphur battery is most attractive from the point of view of abundance and low cost of active materials; its demonstrated cycle life is quite low, however. The most attractive feature of the Zn/Cl_2 battery is its low temperature (50 °C) of operation; its low demonstrated cycle life, hazards of storing chlorine as solid $Cl_2.6H_20$, and the highly corrosive nature of this system are some of its less attractive features; also, the usual problems (*i.e.*, dendrite formation) associated with the recharging of the zinc electrode must be tackled.

Less advanced than the three high energy density battery systems listed in Table 12 are:

(i) Ni–Zn battery

Recently, Gould Batteries has been awarded a $ 5.7 million contract by DOE (Department of Energy, U.S.A.) to work on the research, development and demonstration of this battery for electrical vehicles in the mid-1980s [29]. Problems of dendrite formation on the Zn electrode and fears associated with the introduction of huge quantities of Ni in the general environment are some of the problems.

(ii) Zinc–bromine battery

Exxon has recently [30] demonstrated a prototype with a projected energy density of 77 watt-hours per kg, *i.e.*, about two to three times that of conventional lead–acid batteries. General Electric Company is also working actively on this system [31]. Its most attractive features are low-cost components and ordinary temperatures. Further extensive work is needed to pinpoint its major problems, in addition to the problem of the zinc electrode.

(iii) Lithium–titanium disulphide intercalated batteries

Small batteries of this type (for watches and calculators) are now commercially available. Exxon claims [32] that they will develop storage batteries based on this system. Since this battery uses an organic electrolyte, internal resistance is expected to be high, thus making the exploitation of this system difficult for high load situations, as in storage batteries.

Energy storage by batteries is dependent on the availability of reliable and inexpensive high performance secondary batteries. The common factor that determines the commercial availability of such batteries is the fulfillment of the exacting materials requirements for every one of these batteries. These requirements are varied and complex for each battery system and have been

TABLE 14

The advantages and drawbacks of various contending battery systems [28]

Type	Inherent drawbacks	Advantages	Needed technological advances	Comments
Near-term batteries				
Lead–acid	Low specific energy	Only type available now	None	Best suited for commercial fleets with a range of <100 miles
	Marginal peak power			Environmental problems with lead mining and battery manufacture could be harmful
Nickel/zinc	ZnO_2 dissolves in the electrolyte, shortening battery life	Excellent power and volumetric energy density characteristics	Major improvement in cycle life	Leading candidate for near-term transportation applications. Little nickel is available in U.S.
Nickel/iron	High initial cost	Inherently rugged and long-lived	Reduce gassing during charging	Invented by Edison in 1901; now in mature state of development
	Hydrogen gas is evolved during charging			Nickel shortages would affect more severely than nickel/zinc
Advanced batteries				
Lithium/iron sulphide	Operates at >400 °C	Most compact battery likely to be available by 1990	Long lifetime and high performance not yet achieved in same battery	Most promising of intermediate term batteries
		Safe, even when crushed		First road tests stated for 1979
Zinc/chlorine	Marginal energy efficiency	Materials available and inexpensive	Serious hazard of chlorine release in an accident must be overcome	Better suited for electric utility load levelling than for transportation
	Does not "scale-down" well for vehicle use	Good specific energy and long lifetime appear possible		
Sodium/sulphur	High peak-to-average power ratio requires operation at low energy density Sodium hazard in an accident very great	Materials available and inexpensive	Lower corrosion of positive electrode Improve durability of ceramic electrolyte Establish sodium safety in an accident	Better suited for electric utility load levelling than for transportation

recently reviewed by Battles *et al.* [33]. Some other recent publications dealing with batteries may also be mentioned here [34 - 37].

(C) Photo-electrochemical energy conversion devices

Electrochemical devices also provide a means of converting optical energy either to chemical energy (in photo-electrolysis cells) or to electrical energy (in electrochemical photo-voltaic cells). In practical terms, this optical energy in question is, of course, the solar illumination. A simple photo-electrolysis cell is shown in Fig. 6 [38]. The electrode under illumination must be a semiconductor. In a typical setup (Fig. 6), the anode may be an n-type TiO_2 electrode and the cathode may be made of platinum. When a photon of light is absorbed at the semiconductor electrode (anode in our example), an electron–hole pair is created. The electron and the hole separate under the influence of the electric field at the semiconductor–electrolyte interface. The hole is driven to the anode surface and reacts with OH^- ions to give oxygen. The electrons are conducted through the external circuit to the platinum cathode where they react with protons to give gaseous hydrogen. Low conversion efficiencies (0.5 - 1%) and low stability of the semiconductor electrodes are the main unsolved problems in these devices [39].

Electrochemical photovoltaic cells are true power sources in that the output is electrical energy. They are similar to the photoelectrolysis cells except that only one redox couple predominates in the electrolyte so that the two electrode reactions are the inverse of each other, *i.e.*,

$$\text{Red} + h^+ \longrightarrow \text{Ox}^+ \ (\text{Anode reaction}) \tag{24}$$

and

$$\text{Ox}^+ + e^- \longrightarrow \text{Red (Cathode reaction)} \tag{25}$$

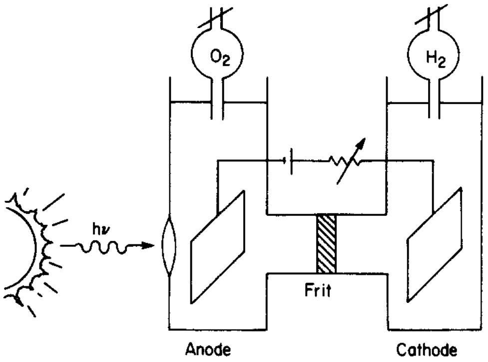

Reactions: $H_2O \xrightarrow{2h\nu} H_2 + 1/2\ O_2$
on the anode: $2h^+ + 2OH^- \longrightarrow 1/2\ O_2 + H_2O$
on the cathode: $2e^- + 2H^+ \longrightarrow H_2$

Fig. 6. Schematic diagram of a photo-electrolysis cell [38].

The electrolyte thus suffers no net chemical change. The absorbed optical energy increases the free energy of electrons in the semiconductor electrode; the useful electrical work is done when these electrons traverse the external circuit to maintain the two electrochemical reactions. Energy conversion efficiencies as high as 10% have been reported for these cells (Table 15). The problems of electrode stability are relatively less severe for these cells.

In addition to the electrochemical stability of the semiconducting surface, there are two other critical parameters for the semiconductor electrodes employed in both these systems: the band gap and the flat-band potential. The band gap determines the absorption characteristics and thence the ultimate conversion efficiency possible in these cells. As regards the flat-band potential, it governs the maximum attainable photo-voltage of electrochemical photo-voltaic cells; for the photo-electrolysis cells, it affects the conversion efficiency by establishing the external bias requirements [38 - 40]. A tabulation of these two parameters critical to the performance of semiconductor electrodes in photo-electrochemical devices has been published by Nozik [39] and is given here in Table 16.

TABLE 15

Maximum experimental efficiency observed for some electrochemical photovoltaic cells; from Nozik [39]. Values followed by parentheses refer to monochromatic conditions

Semiconductor electrode	Predominant redox couple	Maximum experimental efficiency (%)
n-CdS	S^{2-}/S_n^{2-}	1 - 2
n-CdS	Se^{2-}/Se_2^{2-}	3 (5000)
n-CdS	Te^{2-}/Te_2^{2-}	1 (4880)
n-CdSe	S^{2-}/S_n^{2-}	7 - 8
n-CdSe	Se^{2-}/Se_2^{2-}	2 (6330)
n-CdSe	Te^{2-}/Te_2^{2-}	1 - 2 (6330)
n-CdTe	Se^{2-}/Se_2^{2-}	9 (6330)
n-CdTe	Te^{2-}/Te_2^{2-}	10 (6330)
n-CdTe	–	5
n-GaAs	Se^{2-}/Se_2^{2-}	9 - 10
n-GaAs	Te^{2-}/Te_2^{2-}	1 - 3 (6330)
n-InP	Te^{2-}/Te_2^{2-}	1
n-GaP	S^{2-}/S_n^{2-}	–
n-GaP	Se^{2-}/Se_2^{2-}	2 (4550)
n-GaP	Te^{2-}/Te_2^{2-}	1 (4550)
n-Si	$Fe(Cp)_2/Fe(Cp)_2^+$	2 (6330)
n-TiO_2	O_2/H_2O	0.5 - 1
p-MoS_2	Fe^{3+}/Fe^{2+}	1
n-CdS/n-GaAs	S^{2-}/S_n^{2-}	3

TABLE 16

The values of critical semiconductor parameters for materials studied as photoelectrolysis electrodes [39]

Semiconductor electrode*	Band gap (eV)	Flat-band potential** (Volts *vs.* SCE)	pH
n-ZrO_2	5.0	−2.0	13.3
n-Ta_2O_5	4.0	−1.4	13.3
n-SnO_2	3.5	−0.7	13.0
n-$KTaO_3$	3.5	−1.3	13.0
n-$SrTiO_3$	3.4	−1.4	13.0
n-Nb_2O_5	3.4	−1.0	13.3
n-$BaTiO_3$	3.3	−0.8	13.6
n-TiO_2	3.0	−1.0	13.0
p-SiC	3.0	+1.1	14.0
n-V_2O_5	2.8	+0.8	7.0
n-Bi_2O_3	2.8	−0.1	9.0
n-PbO	2.8	−0.3	9.0
n-$FeTiO_3$	2.8	+0.1	14.0
n-WO_3	2.7	+0.2	7.0
n-$WO_{3-x}F_x$	2.7	–	–
n-$YFeO_3$	2.6	−0.5	14.0
n-$Pb_2Ti_{1.5}W_{0.5}O_{6.5}$	2.4	−0.6	13.3
p-ZnTe	2.3	−1.0	14.0
n-$PbFe_{12}O_{19}$	2.3	+1.0	13.3
p-GaP	2.3	+ 0.8	1.0
n-$CdFe_2O_4$	2.3	−0.2	13.3
n-Fe_2O_3	2.2	−0.1	9.0
n-CdO	2.2	−0.2	13.3
n-$Hg_2Nb_2O_7$	1.8	−0.1	13.3
n-$Hg_2Ta_2O_7$	1.8	−0.2	13.3
p-CuO	1.7	+0.3	7.0
p-InP	1.3	−0.1	1.0
p-CdTe	1.4	–	–
p-GaAs	1.4	−0.2	9.2
p-Si	1.1	−0.3	1.0

*Maximum experimental conversion efficiency with sunlight for this group of materials is 0.5 - 1.0%. Semiconductor electrodes having band gaps greater than 3 eV are limited by low solar absorptivity; those with band gaps less than 3 eV have been limited by large bias requirements (unfavorable flat-band potentials).

**Values decrease approximately 0.06 V per unit increase in pH. Values *vs.* SCE are converted to NHE scale by adding + 0.24 volts.

In terms of research effort, as distinct from technological development, photo-electrochemical energy conversion is an area of very considerable current interest. Since the pioneering work of Honda *et al.* [41 - 43], many workers have entered the field and a very rich crop of publications has appeared since about 1975. Detailed references to this work may be found in refs. 4, 38 - 40.

Acknowledgments

Grateful acknowledgment is made to my present and former collaborators (1966 - 1979) for their contributions to my work which has been honoured by the Chemical Institute of Canada through the Noranda Lecture Award. I am especially indebted to Dr. A. Bélanger, Dr. G. Bélanger, Mr. R. Jacques and Dr. J.-P. Randin in this regard. Dr. M. Gauthier is thanked for some general discussions bearing on storage batteries. Dr. K. Dimoff deserves many thanks for discussions on metal/plasma interfaces. Dr. R. Bartnikas and Dr. L. Boulet have been the source of much encouragement and support and I am deeply grateful to them.

References

1 A. K. Vijh, *Electrochemistry of Metals and Semiconductors*, Marcel Dekker, New York, 1973.
2 A. K. Vijh, *J. Chem. Ed.*, *47* (1970) 680.
3 E. S. Casey, *Chem. in Canada, 31* (1) (1979) 28.
4 A. Heller (ed.), *Semiconductor Liquid-Junction Solar Cells*, The Electrochemical Society, Inc., Princeton, N. J., U.S.A., 1977.
5 A. K. Vijh, *J. Chim. Phys., 71* (1975) 812.
6 I. Morcos, *J. Electrostatics, 5* (1978) 51.
7 J. O'M. Bockris and S. Srinivasan, *Nature (London), 215* (1967) 197.
8 P. Stonehart and P. N. Ross, *Catal. Rev., 12* (1975) 1.
9 A. J. Appleby, *Catal. Rev., 4* (1970) 221.
10 M. W. Breiter (ed.), *Proc. Symp. on Electrocatalysis*, The Electrochemical Society, Princeton, N. J., 1974.
11 J. O'M. Bockris and S. Srinivasan, *Fuel Cells and their Electrochemistry*, McGraw-Hill, New York, 1969.
12 B. E. Conway, *Theory and Principles of Electrode Processes*, Ronald Press, New York, 1965.
13 G. Sanstede (ed.), *From Electrocatalysis to Fuel Cells*, University of Washington Press, Seattle, 1972.
14 A. D. Franklin (ed.), Electrocatalysis on Non-Metallic Surfaces, *Nat. Bur. Std. Spec. Publ. 455*, U.S. Government Printing Office, Washington, D. C., 1976.
15 H. Gerischer, in H. Eyring (ed.), *Physical Chemistry: An Advanced Treatise*, Vol. IX A, Academic Press, New York, 1969.
16 M. J. Sparnaay, *Adv. Coll. Interface. Sci., 1* (1967) 277.
17 P. J. Boddy, in H. Reiss (ed.), *Progess in Solid State Chemistry*, Vol. 4, Pergamon, New York, 1967.
18 V. A. Myamlin and Y. V. Pleskov, *Electrochemistry of Semiconductors*, Plenum Press, New York, 1967.
19 A. J. Nozik, *Annu. Rev. Phys. Chem., 29* (1978) 189.
20 A. K. Vijh, *J. Electrochem. Soc., 119* (1972) 1 498.
21 A. K. Vijh, *J. Electrochem. Soc., 119* (1972) 1 187.
22 A. K. Vilh, *Surf. Technol., 4* (1976) 401.
23 A. K. Vijh, *J. Chim. Phys., 72* (1976) 566.
24 E. V. Somers, D. Berg and A. P. Fickett, *Annu. Rev. Energy Sci., 1* (1976) 345.
25 A. P. Fickett, *Sci. Amer.*, Jan. 1979, p. 54.
26 A. P. Fickett, paper presented at the Tenth Annual Meeting of the International Electric Research Exchange (IERE), Toronto, Canada, May 28 - 30, 1979.

27 J. F. Birk, K. Klunder and J. R. Smith, *IEEE Spectrum*, March 1979, p. 49.
28 Anon., *Chem. Eng. News* (Am. Chem. Soc. Publ.), May 7 (1979) 20.
29 Anon., *Ev Focus, 1 (8)*, June 1, (1978) 2, McGraw-Hill Publications (1978).
30 Anon., *Chem. Eng. News* (Am. Chem. Soc. Publ.), Oct. 16 (1978) 21.
31 F. G. Will and H. S. Spacil, *Extended Abstract 14, The Electrochemical Society Meeting (Oct. 1978) Volume*, The Electrochemical Society, Princeton, N. J., 1978.
32 Anon., *Chem. Eng. News* (Am. Chem. Soc. Publ.) Oct. 2 (1978) 14.
33 J. E. Battles, J. A. Smaga and K. M. Myles, *Met. Trans. A, 9A* (1978) 183.
34 J. R. Birks, *EPRI J.*, Oct. (1976) 7.
35 N. P. Yao and J. R. Selman (eds.), *Load Levelling*, The Electrochemical Society, Inc., Princeton, N. J., U.S.A., 1977.
36 F. R. Kalhammer and T. R. Schneider, *Annu. Rev. Energy, 1* (1976) 311.
37 E. Hollax, *J. Power Sources, 4* (1979) 11.
38 M. Tomkiewicz and H. Fay, *Appl. Phys., 18* (1979) 1.
39 A. J. Nozik, *Annu. Rev. Phys. Chem., 29* (1978) 189.
40 K. Rajeshwar, P. Singh and J. Dubow, *Electrochim. Acta, 23* (1978) 1 117.
41 A. Fujishima, K. Honda and S. Kikuchi, *J. Chem. Soc. Jpn., 72* (1969) 108.
42 A. Fujishima and K. Honda, *Bull. Chem. Soc. Jpn., 44* (1971) 1 148.
43 A. Fujishima and K. Honda, *Nature (London), 238* (1972) 37.